

6-2006

Real-time identification of sliding friction using LabVIEW FPGA

Laine Mears

Clemson University, mears@clemson.edu

Jeannie S. Falcon

IEEE

Thomas R. Kurfess

IEEE

Follow this and additional works at: https://tigerprints.clemson.edu/auto_eng_pub



Part of the [Automotive Engineering Commons](#)

Recommended Citation

M. L. Mears, J. S. Falcon and T. R. Kurfess, "Real-time identification of sliding friction using LabVIEW FPGA," 2006 American Control Conference, Minneapolis, MN, 2006, pp. 6 pp.-.

This Conference Proceeding is brought to you for free and open access by the Automotive Engineering at TigerPrints. It has been accepted for inclusion in Publications by an authorized administrator of TigerPrints. For more information, please contact kokeefe@clemson.edu.

Real-Time Identification of Sliding Friction Using LabVIEW FPGA

M. Laine Mears, Jeannie S. Falcon, *IEEE*, and Thomas R. Kurfess, *IEEE*

Abstract—Friction is present in all mechanical systems, and can greatly affect system stability and control in precision motion applications. In this paper, we present application of a frictional model to trajectory planning of a part centering system with Real-Time identification of model parameters through system force and position response. This identification is carried out using LabVIEW Motion Control software and Digital Signal Processing (DSP) and Field-Programmable Gate Array (FPGA) hardware. A comparison of hardware performance for force measurement is also made.

I. INTRODUCTION

MOTION control of frictional systems has been extensively studied due to inherent difficulties of modeling and compensation of nonlinear frictional effects. A number of friction models and compensation schemes have been developed to describe these effects in the context of positioning [1], [3], [6]. Recently, a greater focus on sliding dynamics and positioning by sliding has been studied as a lower cost and more flexible actuation alternative to traditional robotic positioning [4], [5], [7].

Issues of frictional controller design and appropriate selection of the underlying friction model are important. Equally important is the understanding that friction is a time-varying phenomenon, and can change dramatically with wear or introduction of contaminants to the system. It is therefore necessary to be able to continuously quantify the frictional state of a system to provide optimal motion control.

This work presents a real-time friction identification scheme for sliding, implemented through a dedicated real-time motion control system utilizing DSP for motion control and FPGA for force data collection and analysis.

II. SYSTEM MODEL DEVELOPMENT

The first activity is to understand the system dynamic response through creation of a system model.

A. Prototype Application

The application under study is ring centering on a rotating

plate through constant-velocity actuation by a pushing element. The system is shown in Figure II.1:

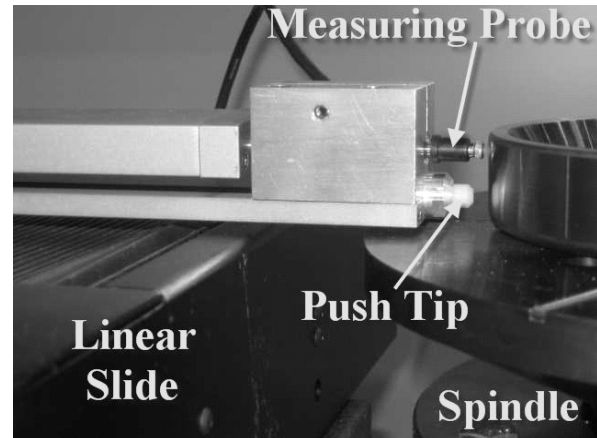


Fig. II.1 - Prototype System Components

The measurement probe commands the linear slide servo following, and also gathers data for characterization of the ring surface. The data are modeled through a least-squares technique, and then parameters such as offset distance and direction are extracted from the model. These parameters are directed to a motion control subprogram that actuates the slide at constant velocity in such a manner to cause the push tip to move the part geometric center in line with the center of rotation. As the part is actuated, force data is collected from a piezoelectric sensor in the push tip. The target tolerance for alignment of centers is $2.5 \mu\text{m}$.

The system is implemented on a National Instruments PCI with Extensions for Instrumentation (PXI) Real-Time control system, integrating a PXI-8187RT controller, PXI-7350RT motion control module, and a PXI-7831R FPGA module. The PXI-7350RT uses both an onboard Motorola 68331 floating point processor and an onboard Digital Signal Processor (DSP) for 8-axis motion control (3 utilized in this application). The FPGA is utilized for force sensor data acquisition due to the high available sampling rate, and is programmed using the LabVIEW FPGA software module. All hardware components are integrated in a common PXI chassis.

B. Frictional Modeling

The sliding system is idealized as a simple second-order relative model as shown in Figure II.2:

Manuscript received March 24, 2006. This work was supported in part by grants and test equipment from National Instruments Corporation and The Timken Company.

M. L. Mears is a Ph.D. Candidate with Georgia Institute of Technology, Atlanta, GA 30332 USA. (404 386 4178; lmears@pmrc.marc.gatech.edu).

J. S. Falcon is a Senior Engineer in the Control and Simulation department of National Instruments Corporation, Austin, TX 78712 USA (jeannie.falcon@ni.com).

T. R. Kurfess is BMW Chair in Manufacturing and Director of the Campbell Graduate Engineering Center, Clemson University, Clemson, SC 29634 USA (kurfess@clemson.edu).

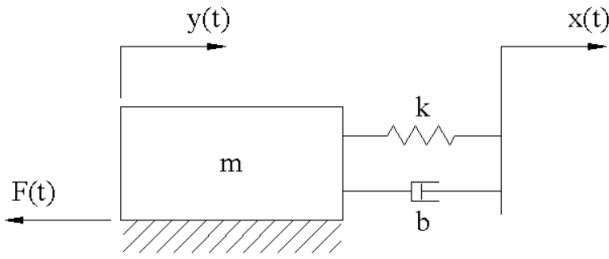


Figure II.2 - Idealized System with Friction

Friction is modeled using the viscous Coulomb form, which incorporates separate descriptions of frictional force depending on velocity state of the mass. The friction is described by [1]:

$$F(t) = \begin{cases} \mu_k F_N + k_v v & , v \neq 0 \\ F_e & , v = 0 \text{ and } |F_e| < F_S \\ F_S & , \text{otherwise} \end{cases}$$

$\mu_k \equiv$ kinetic friction coefficient
 $F_N \equiv$ part normal force
 $F_e \equiv$ applied force
 $F_S \equiv$ static friction force = $\mu_s F_N$

The overall system is described by the governing equation

$$m\ddot{x} + b(\max(\dot{y} - \dot{x}, 0)) + k(\max(y - x, 0)) = -F(t)$$

This model accounts for unidirectionality of the spring and damping idealized elements in the pushing application.

Model parameters are selected and the model validated for a clean, dry system. Modeled position and force response plots are shown in Figure II.3 and Figure II.4 respectively.

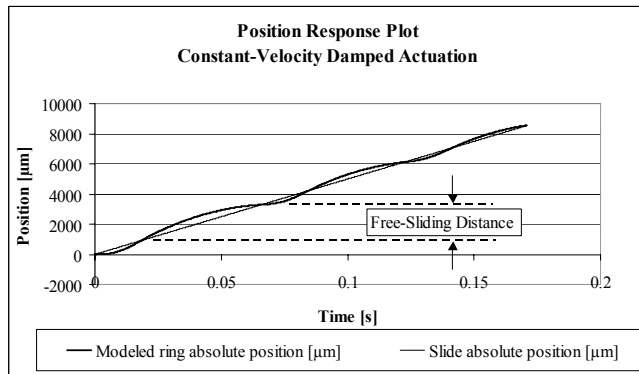


Fig. II.3 - Position Response, m=18.9 kg, v=3000 mm/min

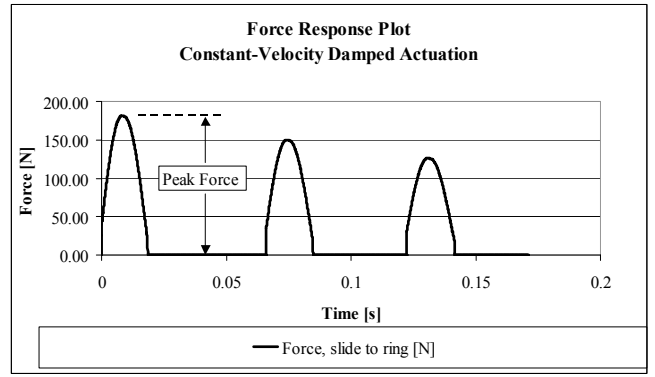


Fig. II.4 - Force Response, m=18.9 kg, v=3000 mm/min

For each plot, a characteristic dimension is defined, which is to be used in the subsequent friction predictor model. *Free-sliding distance* d is defined for position response as the distance the part travels from loss of contact with the actuator until coming to a stop under the influence of friction. For force response, the *peak force* F_p is defined as the maximum force observed over the actuation.

C. Friction Identification

The preceding friction model is constructed using static friction parameters derived and validated from dry sliding experiments. However, in practice system frictional state is seldom constant. Wear of sliding surfaces, transport of solid and liquid contaminants into and out of the system, and variations in the condition of parts being centered all introduce variation into the friction model.

To capture these effects, a real-time identification scheme of underlying friction model parameters is described. Identification of the primary friction model parameters is treated in [2] using a log decrement method. In this work, identification is undertaken through inversion of the general dynamic model with respect to peak force achieved per actuation and to free-sliding distance achieved. In this way, a single actuation can provide a friction estimate from separate sources.

1) Force Model

The centering prototype machine includes an analog piezoelectric force sensor of range ± 446 N and sensitivity of 11.2 mV/N. During actuation, force is measured in real time. Observed peak force for a given set of actuation conditions (i.e., actuation velocity, part attributes, measured friction coefficient) is used to validate the initial system model given by (2). This model is then used to generate a family of curves relating expected peak force F_p to actuation velocity and static friction coefficient μ_s . For purposes of simplifying the model, the kinematic friction coefficient μ_k to assumed to be 75% of the static coefficient, a relationship observed over the velocity range tested. The curve family generated by this method for a part of 18.9 kg is given in Figure II.5.

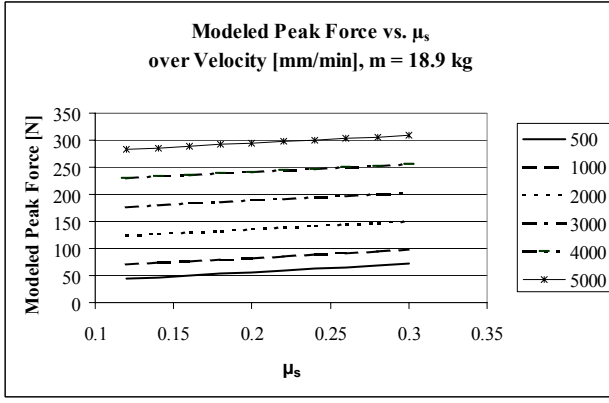


Fig. II.5 - Peak Force Model

The curves are fit to a linear model in v and μ_s :

$$F_p = C_v v + C_\mu \mu_s \quad (3)$$

Coefficients of this model are computed through a least squares fitting routine and the model inverted to determine an expression for the static friction coefficient:

$$\mu_s = \frac{F_p - 0.0529v}{146.2}$$

$$F_p = \text{measured peak force [N]} \quad (4)$$

$$v = \text{actuation velocity} \left[\frac{\text{mm}}{\text{min}} \right]$$

2) Distance Model

The free sliding distance predicted by (2) is validated through experiment. The model is then used to generate a family of curves relating free-sliding distance d to actuation velocity v and static coefficient of friction μ_s . The curve family is shown in Figure II.6 for an 18.9 kg part.

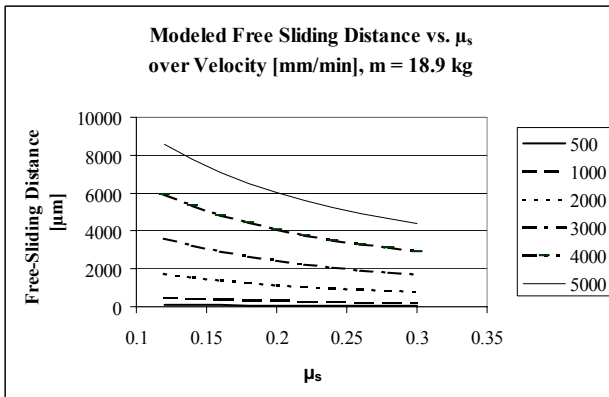


Fig. II.6 - Free-Sliding Distance Model

The model is reduced to a second-order parabolic form, with coefficients assumed of the power form in velocity:

$$d - d_0 = A(\mu_s - \mu_0)^2$$

$$d_0 = C_1 v^{k_1} \quad (5)$$

$$A = C_2 v^{k_2}$$

This model is fit to the observed data and inverted to arrive at an expression for prediction of the static friction coefficient:

$$\mu_s = 0.3415 - \sqrt{\frac{d - 0.00041v^{1.8997}}{0.07379v^{1.6428}}}$$

$$d \equiv \text{free sliding distance} [\mu\text{m}] \quad (6)$$

$$v \equiv \text{slide velocity} \left[\frac{\text{mm}}{\text{min}} \right]$$

3) Optimal Combined Estimator

The two friction predictor sources are combined through a weighting scheme proportional to the sensitivity to friction model parameters at the operating point in question. Referring to Figure II.6, when velocity is lower (e.g., 500 mm/min), the distance response is insensitive to variation in the friction parameter. However, at larger actuation velocities (> 2000 mm/min), sensitivity increases. For this reason, the derivatives of the force and distance functions at the system operating point are used as weights in the combined predictor. Additionally, the distance parameter is normalized to force units over the entire range examined:

$$\mu_s^* = \mu_{s,force} \frac{\frac{\partial F}{\partial \mu}}{\frac{\partial F}{\partial \mu} + \frac{\partial d}{\partial \mu} \frac{\Delta F}{\Delta d}} + \mu_{s,dist} \frac{\frac{\partial d}{\partial \mu} \frac{\Delta F}{\Delta d}}{\frac{\partial F}{\partial \mu} + \frac{\partial d}{\partial \mu} \frac{\Delta F}{\Delta d}} \quad (7)$$

This optimal combination gives higher weight to the predictor with greater model sensitivity to changes in the friction parameter.

III. IMPLEMENTATION

The friction identification scheme is implemented on the single-actuator centering prototype.

A. Force Sensing

Force sensing is accomplished through a piezoelectric sensing element whose output is amplified and directed to the analog input (AI) port of the FPGA PXI-7831R card mounted in the PXI real-time system chassis. Force capture occurs through FPGA AI capture as shown in Figure III.1.

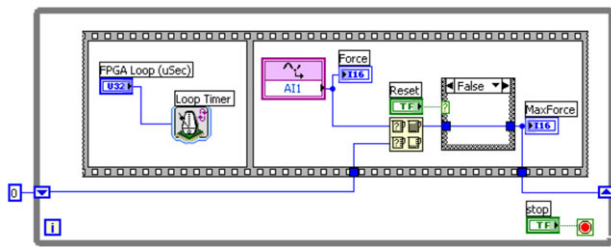


Figure III.1 - Data Acquisition Code for Force on FPGA

Force is continually acquired at a rate set by the FPGA loop timer. Peak force reading is maintained for each individual actuation.

The FPGA data are passed to the real time operating system by way of an acquisition loop as shown in Figure III.2.

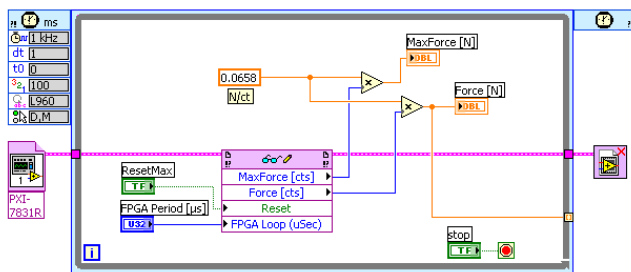


Figure III.2 - Real-Time Force Signal Processing

The acquired force is passed to the real-time motion control loop for display and use in trajectory planning. A sample trace of force over two actuation strokes is shown in Figure III.3. The largest peak shown begins the second actuation.

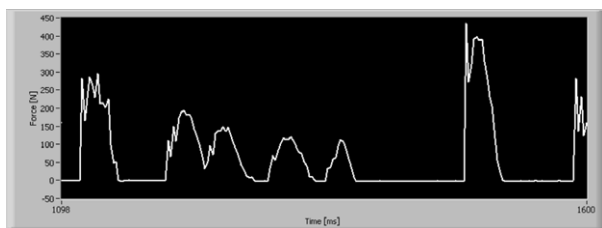


Figure III.3 - Force Data Collection

B. Distance Sensing

The free-distance utilized in the friction predictor model is quantified by a digital linear measurement probe that creates a quadrature encoder signal with resolution of 20 nm. The probe output is captured from the point of loss of contact as read from the actuation force sensor until the part has stopped sliding. The probe output is directed to a digital encoder input of the DSP module.

IV. RESULTS

A. Prediction Accuracy

The prediction scheme is applied to pushing actuation and

sliding response of the part shown in Figure IV.1 on a table with 3 x 1 mm carbide rails. The part is nonrotating and initially at rest. Two conditions are tested:

- DRY: table and part are cleaned and dried
- OILY: DTE Medium oil is applied to sliding surfaces



Figure IV.1 - Sample Part Under Test, m=18.9 kg

The static friction breakaway force is tested using a hand gauge at low velocity and found for each condition to be

DRY: $\mu_s = 0.141$

OILY: $\mu_s = 0.135$

1) Force Model

The part is actuated over a range of constant velocities. For each trial, the peak force is measured and the static friction coefficient calculated from (4). Results of the force predictor are shown in Table 1 for DRY condition and Table II for OILY condition.

TABLE I
FRICTION PREDICTOR RESULTS USING PEAK FORCE - DRY

Actuation Velocity (mm/min)	Peak Force (N)	μ_s Predicted	Error to Measured μ_s
500	46.1	0.134	-4.3%
1000	80.2	0.187	32.8%
2000	127.3	0.147	4.5%
3000	181.0	0.152	8.5%
4000	232.0	0.139	-0.8%
5000	283.9	0.133	-5.5%

TABLE II
FRICTION PREDICTOR RESULTS USING PEAK FORCE - OILY

Actuation Velocity (mm/min)	Peak Force (N)	μ_s Predicted	Error to Measured μ_s
500	42.1	0.107	-19.9%
1000	79.7	0.183	34.3%
2000	136.3	0.209	52.5%
3000	183.7	0.171	25.7%
4000	236.8	0.172	26.7%
5000	285.9	0.147	8.3%

Force prediction is more accurate in the dry condition.

2) Distance Model

For the actuation trials, the free-sliding distance is also measured using the distance probe. For each trial, the static friction coefficient is estimated by (6). Results of the distance predictor are given in Table III for DRY condition and Table IV for OILY condition.

TABLE III
FRICTION PREDICTOR RESULTS USING SLIDING DISTANCE - DRY

Actuation Velocity (mm/min)	Sliding Distance (μm)	μ_s Predicted	Error to Measured μ_s
500	265	0.018	-87.4%
1000	613	0.086	-38.6%
2000	1240	0.186	32.1%
3000	2844	0.165	17.1%
4000	5215	0.145	3.1%
5000	8175	0.133	-5.1%

TABLE IV
FRICTION PREDICTOR RESULTS USING SLIDING DISTANCE - OILY

Actuation Velocity (mm/min)	Sliding Distance (μm)	μ_s Predicted	Error to Measured μ_s
500	267	0.016	-84.3%
1000	590	0.193	-29.5%
2000	1240	0.186	36.1%
3000	2875	0.162	19.5%
4000	5475	0.134	-0.4%
5000	8620	0.122	-9.5%

As expected from Figure II.6, the distance predictor is more accurate at higher velocities. This effect is accounted for in the weighting scheme of (7).

3) Optimal Combined Estimator

The estimator of (7) is applied to the force- and distance-based friction predictor results. Results of a single trial at $v=5000$ mm/min are given in Table V.

The predictor is accurate to within approximately 5% in

TABLE V
WEIGHTED FRICTION PREDICTOR RESULTS, $v=5000$ MM/MIN

Condition	μ_s Measured	μ_s Predicted	Error to Measured μ_s
DRY	0.141	0.133	5.2%
OILY	0.135	0.131	2.9%

the worst case.

B. FPGA Performance

The sampling of force using FPGA is compared to sampling of force through the analog (AI) port of the Digital Signal Processor (DSP) motion control card used for actuator control. A single point AI force acquisition loop is written and thread execution time monitored.

1) Force Sampling by DSP

Force acquisition occurs at an average execution time of 1010 μs on the DSP hardware, equivalent to a sampling rate of 990 Hz. Additionally, if the force acquisition is run in parallel with other threads such as motion control and data analysis, the force acquisition task will share processor time and be subject to prioritization and preemption rules. This situation will tend to increase the average loop time.

2) Force Sampling by FPGA

FPGA force acquisition is run in a separate thread on the FPGA module, so is not subject to real-time controller preemption. Average data acquisition time for a single AI sample loop is 4.3 μs , equivalent to a reliable sampling rate of 200 kHz when accounting for additional software overhead.

Sample rate is improved by a factor of more than 200 by using FPGA hardware over DSP hardware for force sampling.

V. CONCLUSIONS

This paper describes a methodology for developing a friction prediction expression for sliding in terms of observed peak force and free-sliding distance under constant-velocity actuation. This methodology demonstrated for a specific part on a specific system can be repeated and validated for any combination of system setup. Implementation is carried out using an FPGA module configured for data collection and analysis, housed in a Real-Time controller chassis.

A. Friction Identification

A first-order friction predictor from observed force and a second-order friction predictor from observed free-sliding distance was introduced. Additionally, a derivative-

weighted combination scheme was defined. The identification scheme predicted sliding friction in the given application to within 5%.

This friction identification methodology also has implications beyond system modeling and motion control path planning. Additionally, real-time friction identification can be used as an element in machine diagnostic evaluation. The vision is to monitor machine health through detection of significant changes in system frictional state and to provide subsequent generation of maintenance requests or alarm conditions.

B. FPGA

Collection of force data through both DSP and FPGA sampling was carried out and execution time of each scenario measured. Sample rate using FPGA not only outperformed sampling using DSP by a factor of over 200, but also liberated processor resources that could be applied to other time critical tasks, improving the overall effectiveness of the system.

Additionally, analog input channels on the FPGA board are independently sampled using separate analog to digital (A/D) converters, compared to the 8-channel single A/D multiplexed operation of the 7350 motion control board.

A future plan for system improvement is performing motion control tasks directly on the FPGA through the LabVIEW SoftMotion module. This is expected to not only increase control loop sample rate, but to also allow for exploration of alternative low-level control schemes in the centering application.

ACKNOWLEDGMENT

This research was made possible by financial and equipment grants from National Instruments corporation and The Timken Company.

REFERENCES

- [1] Åström, K. "Control of Systems with Friction." Technical paper. Department of Automatic Control, Lund Institute of Technology, 1998.
- [2] Feeny, B. and J. Liang. "A Decrement Method for the Simultaneous Estimation of Coulomb and Viscous Friction." *Journal of Sound and Vibration*, v195, n1, Aug, 1996: 149-154.
- [3] Hirschorn, R.M. and G. Miller. 1998, "Control of Nonlinear Systems with Friction." *IEEE Transactions on Control Systems Technology*, v7, n5, Sep, 1999: 588-595.
- [4] Lynch, K. "Estimating the Friction Parameters of Pushed Objects." *1993 International Conference on Intelligent Robots and Systems*, 1993: 186-193.
- [5] Lynch, K. and M. Mason. "Stable Pushing: Mechanics, Controllability, and Planning." *The International Journal of Robotics Research*, v15, n6, Dec., 1996: 533-556.
- [6] Olsson, H., K.J. Åström, C. Canudas de Wit, M. Gafvert and P. Lischinsky. "Friction models and friction compensation." *European Journal of Control*, v4, n3, 1998: 176-195.
- [7] Peshkin, M.A. and A.C. Sanderson. "The Motion of a Pushed, Sliding Workpiece." *IEEE Journal of Robotics and Automation*, v4, n6, Dec., 1988: 569.